Fabrication of high-aspect-ratio double-slot photonic crystal waveguide in InP heterostructure by inductively coupled plasma etching using ultra-low pressure

Kaiyu Cui, Yongzhuo Li, Xue Feng, Yidong Huang, and Wei Zhang

Citation: AIP Advances **3**, 022122 (2013); doi: 10.1063/1.4793082

View online: http://dx.doi.org/10.1063/1.4793082

View Table of Contents: http://aipadvances.aip.org/resource/1/AAIDBI/v3/i2

Published by the American Institute of Physics.

AIP ADVANCES **3**, 022122 (2013)

Fabrication of high-aspect-ratio double-slot photonic crystal waveguide in InP heterostructure by inductively coupled plasma etching using ultra-low pressure

Kaiyu Cui,[a] Yongzhuo Li, Xue Feng, Yidong Huang,[b] and Wei Zhang
Department of Electronic Engineering, Tsinghua National Laboratory for Information Science and Technology, Tsinghua University, Beijing 100084, China

(Received 14 November 2012; accepted 6 February 2013; published online 26 February 2013)

Double-slot photonic crystal waveguide (PCW) in InP heterostructure is fabricated by inductively coupled plasma (ICP) etching. Due to using an ultra-low pressure of 0.05 Pa, etch depths up to 3.5 μm for holes with diameter of 200 nm and 1.8 μm for slots of ~40 nm are achieved, which indicate a record-high aspect-ratio, i.e. 45, for such narrow slots in InP heterostructure. Moreover, etching quality is evaluated based on both the transmission performance and the linewidth of micro-photoluminescence (μ-PL). In our measurement, a structure-dependent transmission-dip about 17 dB is obtained from a 17-μm-long W3 PCW, and a PL widening as small as 19 nm compared to the corresponding wafer is observed. These promising experimental results evidence the high etching quality realized in this work and confirm the feasibility of etching small-feature-size patterns by ICP technology for InP based devices in future mono-/hetero-integrated photonic circuits. [http://dx.doi.org/10.1063/1.4793082]

I. INTRODUCTION

Planar photonic crystal (PhC) of InP-based semiconductor has been an attractive solution to light sources for on-chip optical communications[1–4] due to its innovative properties, such as photonic band gap (PBG), high Q cavity with a small mode volume, and slow light effect. For planar PhC, lightwave is confined by the combining mechanism of in-plane PBG and vertical total internal reflection.[5,6] Thus, planar PhC with InGaAsP active layer sandwiched between InP claddings are either *membrane-type structure* with high index-contract suspend membrane or *substrate-type structure* with low index-contract thick heterostructure.[7,8] The membrane-type PhC can be fabricated by just etching a few hundred nanometres of slabs and a post-wet etching, but it is rather fragile and suffers from bad heat dissipation. Especially, the electrical injection of suspend membrane remains a challenge, and only a few works are realized by lateral PN injection until recently.[9,10] On the contrary, the substrate structure can maturely form a vertical PN junction during the epitaxial process and offers a much stronger mechanical strength as well as a better heat dissipation. Therefore, substrate-type PhC is well suitable for high performance electrically pumped light source. However, due to the low index-contract, the confined mode in InP/InGaAsP/InP heterostructure extends larger than 2 μm.[11] In order to reduce the out-of-plane leakage, InP based micro-/nano-structures must be etched deeply, namely high-aspect-ratio etching technology is essential.[12–14] Obviously, for deep etching, the smaller the openings size is, the more difficult the reaction species escape from the holes, accordingly bringing out a much bigger challenge. What is more, this challenge has be stressed by an emerging interests on slot waveguides[15] with fascinating applications on quantum electrodynamics(QED),[16] nonlinear optics,[17] bio-sensing,[18,19] optomechanics[20]

[a]Electronic mail: kaiyucui@tsinghua.edu.cn.
[b]Electronic mail: yidonghuang@tsinghua.edu.cn.

and enhancement of light-matter interaction,[21] since such slotted structures confines and guides light in low-index slot region with nanoscale dimension so that ultra-small mode volume can be achieved.[22]

In these regards, for hole diameter in the range of 300∼500 nm, etch depths up to 4∼5 μm have been achieved by chemically assisted ion beam etching (CAIBE)[23,24] or by inductively coupled plasma reactive ion etching (ICP-RIE).[12,25] While, for holes with diameter around 200nm, reported etch depths are mainly about 3 μm.[11,12,24,25] To date, the best-reported result for InP-based PhC etching is attained by CAIBE technology, which etch depth (aspect-ratio) of 5.3 μm (21) and 3.5 μm (38) for holes with diameter of 250 nm and slots of 90 nm was achieved, respectively.[14] However, compared with CAIBE technology, ICP-RIE is a more versatile etching technique for large scale integration because of a high-density plasma generation and a separate control of ion flux and ion energy, which enables high-aspect-ratio etching in a much shorter time. Therefore, ICP deep etching for small feature size patterns in InP-based material should be further developed.

In this paper, high-aspect-ratio ICP etching of double-slot photonic crystal waveguide (PCW) in InP-based material is demonstrated by exploiting an ultra-low process pressure. Here the double-slot PCW defined in our previous work[26,27] is formed by introducing two slots into a W3 PCW for improving the mode characteristics and taking shape the confinement structure of lateral current diffusion. Since the probability of the species escaping from the holes and slots can be enhanced at low pressure, etch depth larger than 3.5 μm and 1.8 μm for the holes with diameter of 200 nm and the slots of only ∼40 nm are achieved at an ultra-low pressure of 0.05 Pa, respectively. This experimental result indicates that record-high aspect-ratio of 45 for slots narrow to ∼40 nm is achieved. Moreover, etching quality is evaluated by measuring the transmission performance and the micro-photoluminescence (μ-PL) of the etched W3 PCWs. Transmission dip about 17 dB is obtained by the PCW with length of only ∼17 μm. In addition, μ-PL linewidth is only 19nm larger than that of the corresponding wafer. These promising experimental results evidence the high etching quality in this work and confirm the feasibility of etching small-feature-size patterns by ICP technology for InP based devices in future mono-/hetero- integrated photonic circuits.

This article is structured as follows. We first discuss the fabrication results: experimental conditions and fabrication process are addressed at the beginning, and then the impact of the process pressure and the selectivity versus the SiO_2 mask are illustrated. After that, we evaluate the etching quality based on both the transmission performance and the μ–PL linewidth of the etched W3 PCWs.

II. FABRICATION RESULTS

A. Experimental conditions and fabrication process

The structure studied in this work involves two types of PCWs. One is the typical W3 PCW, which is a line-defect PCW with three rows of holes missing. The other one is the double-slot PCW[26,27] formed by introducing two slots into the W3 PCW. Here, the W3 PCW is used for evaluating the etching quality as the approach proposed in Ref. .28 While, etching performance for both holes and slots is investigated via the double-slot PCW.

The fabrication process requires several steps: First, PCW patterns were defined by electron beam-lithography using ZEP-520A as the resist mask and then transferred into a 300-nm-thick SiO_2 hard mask by ICP etching using CHF_3 and Ar mixture. After forming the mask, InP-based PCWs are fabricated by ICP etching with Cl_2 and $SiCl_4$ mixture. At last, the SiO_2 mask was removed from the wafer after InP etching to analyze the etching profiles by the scanning electron microscope (SEM).

The parameters used in the ICP etching are summarized in Table I. The etching conditions are set to accelerate the desorption of reaction products due to the features of InP etching using Cl_2 and its family. As the main reaction products are PCl_3 and $InCl_3$, however, $InCl_3$ is not easy to be volatile owing to its very low vapour pressure.[29,30] The residual $InCl_3$ will redeposit and in turn stop further reaction especially for the case of etching small features, since the reaction species also face the

TABLE I. ICP etching parameters.

Parameters	Value	Unit
Temperature, T	230	°C
Cl_2 flux	1	sccm
$SiCl_4$ flux	3	sccm
Bias power, P_{bias}	260	W
ICP power, P_{ICP}	220	W
Pressure, P	0.05	Pa
Etching time, t	6	minute

difficulty of escaping from the small opening with reduced solid angle of the escape cone.[31] Thus, enhancing the desorption of $InCl_3$ is crucial for high-aspect-ratio etching of ultra-small patterns in InP. Based on this principle, we choose $SiCl_4$ together with Cl_2 in our process which can take advantage of the heavy ionic $SiCl_4$ particles by bombarding the reaction particles efficiently[32] and heat the surface by cracking it. Besides this, we also heat the wafer to a temperature of 230 °C to strengthen desorption of the reaction products.

B. Impact of the process pressure

As is known, for deep etching of small features, the main difficulty is that the reaction species are hard to escape from the small openings without collision. Another severe issue for InP ething using Cl_2 is the low vapour pressure of $InCl_3$ as described above. Thus, if the pressure is decreasing, the mean free path of the species will be larger so that the collision probability will be greatly reduced. Moreover, the low pressure is also beneficial for desorption of $InCl_3$. Based on these insights, we investigate the impact of the process pressure on the etching results. Figure 1 presents the etching results of InP bulk material under different pressures while the ICP power is fixed at 280W and other parameters are consist with the values given in Table I. The hole diameter and slot width of the etched double-slot PCW with lattice period of 400nm is ∼200 nm and ∼50 nm, respectively. It can be seen that while the pressure, P, decreases form 0.15 Pa to 0.05 Pa, the etch depth notably increases as expected. This clear increase in etch depth confirms the effectiveness of using low pressure for small feature size etching in InP. We believe that this approach could pave the wave for the deep etching technique of ultimate feature size patterns.

Then, etching using ultra-low pressure of 0.05 Pa is applied to the fabrication of double-slot PCW and slots with different widths in InP/InGaAsP/InP heterostructure. Figure 2 shows the SEM cut view of the etched sample. The used etching parameters are given in Table I. For our sample, the heterostructure consists of an InGaAsP active layer embedded in InP wafer. Here, multi-quantum wells (MQWs) sandwiched between two 100 nm-thick InGaAsP claddings compose the highlighted active region in Fig. 2.

As can be seen from Fig. 2, PhC holes with diameter of 200nm are etched to depth of ∼3.5 μm. While for the slots with width in range of 40∼430 nm, etch depth larger than 1.8 μm is obtained. Here the slot width is measured along the upper boundary of the active layer to avoid the slightly broadening at the top openings transferred from the distortion of mask erosion during etching.[12] It should be mentioned that using SEM, a slot width can only be measured with an accuracy of about ±5 nm. Moreover, etch depth decreases while the slot becomes narrower. This feature-size dependent effect has also been found in Ref. 24. Despite this, the slot narrow to ∼40 nm is still etched to ∼1.8 μm due to using the low pressure of 0.05 Pa. Thus, aspect-ratio as high as 45 is achieved for the ultra-narrow slot, corresponding a best-reported result up to now for InP etching. This promising result also confirms the feasibility of etching small-feature-size patterns by ICP technology for InP based devices. In addition, high quality and high-aspect-ratio etching of such narrow slot is significant not only for breaking through the limit of the etching technology, but also for future on-chip photonic circuits with ultrahigh integration density.

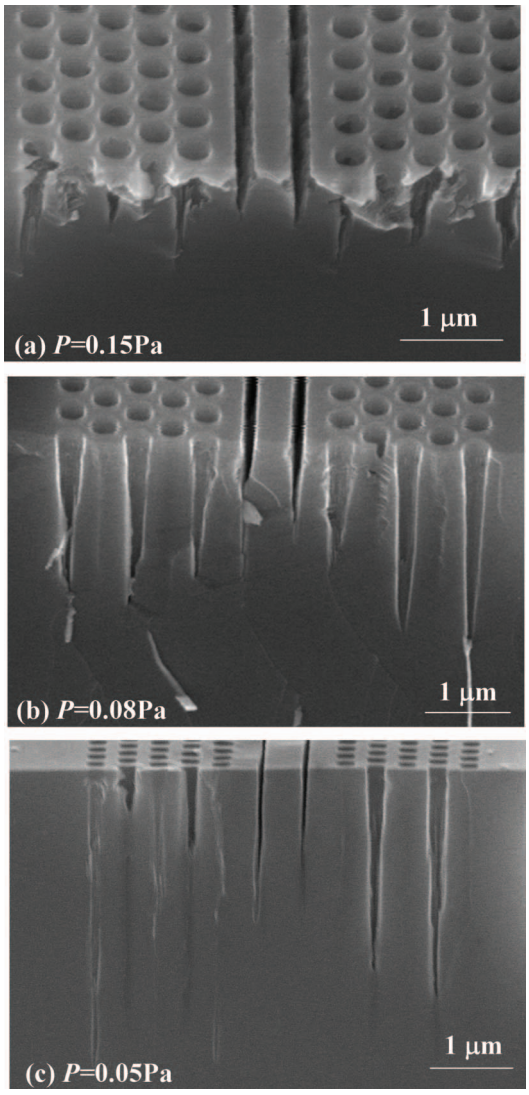

FIG. 1. Role of the process pressure: etched profiles of double-slot photonic crystal waveguides (PCWs) in InP bulk material under pressures of (a) $P = 0.15$ Pa, (b) $P = 0.08$ Pa, and (c) $P = 0.05$ Pa. While the ICP power is fixed at 280W and other parameters are consist with the values given in Table I.

C. Selectivity versus the SiO_2 mask

Besides the etch profile, another concerned figure of merit for ICP etching is the selectivity versus the mask. The selectivity for our etching process (InP etch rate/SiO_2 mask etch rate) is investigated based on two samples, which are etched for 3 minutes and 4 minutes with the same etching condition (given in Table I). The corresponding results with remaining SiO_2 mask are presented in Fig. 3. By measuring the remaining thickness of the SiO_2 mask, etch rate of ~53 nm/min for the SiO_2 mask can be deduced. Taking the etch depth of InP in to account, the etch rate for InP is about 669~788 nm/min. Noticeably, such etch rate for the InP based holes with diameter about ~200 nm is much larger than that achieved by CAIBE,[24] which shows the competitive advantage of ICP technology compared with CAIBE. Finally, based on the ratio of InP etch rate to the SiO_2 mask etch rate, the selectivity is about 14 ± 1 for our etching condition, which is favourable for the deep etching technology.

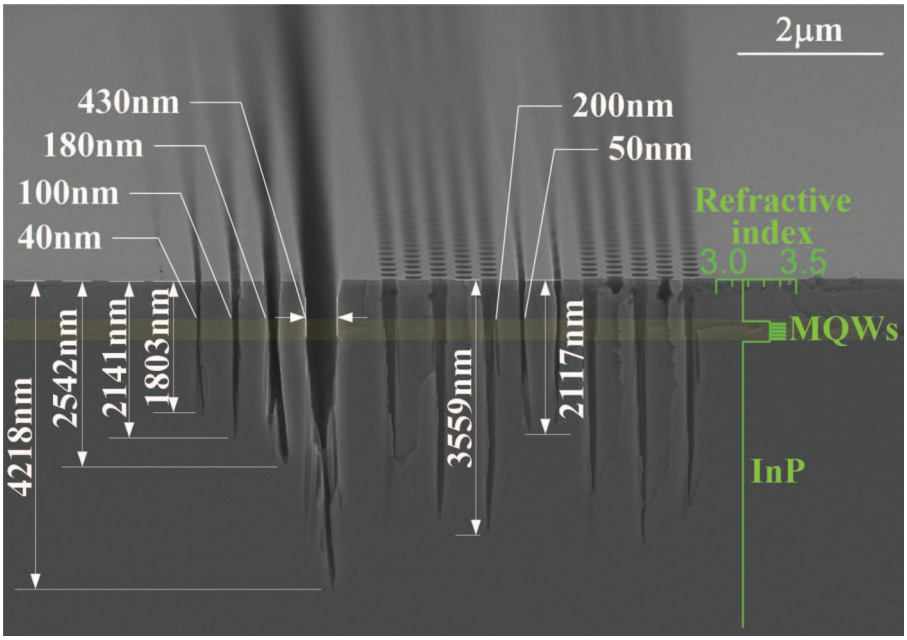

FIG. 2. SEM cut view of double-slot PCW and slots with different widths in InP/InGaAsP/InP heterostructure. The etching parameters are given in Table I.

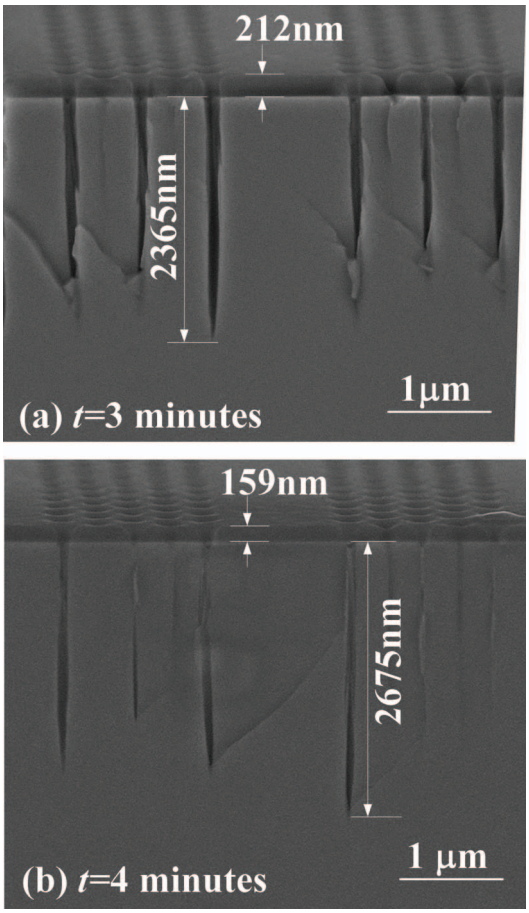

FIG. 3. Selectivity versus the SiO_2 mask: SEM cut views of two PCWs in InP bulk material etched for (a) $t = 3$ minutes and (b) $t = 4$ minutes with the same etching condition given in Table I.

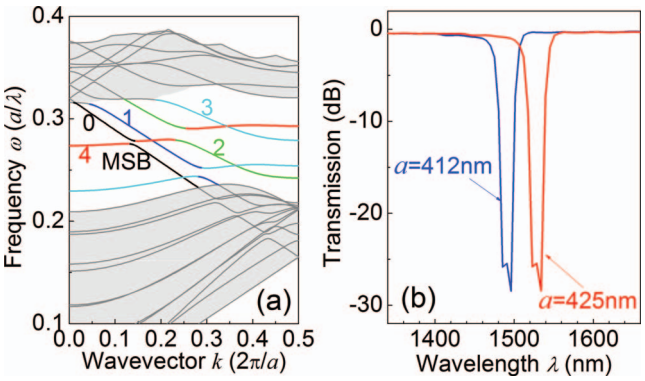

FIG. 4. (a) Transverse electric (TE) mode band structure of the W3 PCW and (b) corresponding transmission spectra for different lattice periods: $a = 412$ nm and $a = 425$ nm.

III. EVALUATION OF ETCHING QUALITY

A. Transmission performance of the etched W3 PCW

To evaluate the etching quality, measuring the fabricated device performance is obviously a straightforward method. In this work, transmission dip of W3 PCW is measured and used for determine the etching quality. Here, we fabricate W3 PCW with a fixed $r/a = 0.345$ (r and a denotes the radius of the PhC holes and the lattice period, respectively.) and two different lattice periods: $a = 412$ nm and $a = 425$ nm, so that the structure-dependent transmission-dip as a clear evidence for the feature of PCW can be predicted.

The band structure and transmission spectra of the W3 PCW are provided in Fig. 4, which are calculated by two dimensional (2D) plane wave expansion (PWE) method and 2D finite-difference time-domain (FDTD) method, respectively. The effective refractive index is set as $n_{\text{eff}} = 3.17$ and r/a consists with the fabrication samples. Due to the unique guiding mechanism of PBG effect, PCW offers the possibility to guide light in the line defect waveguide and Bragg couplings between the defect modes.[33] It can be seen from Fig. 4(a) that there is mode coupling between the fundamental mode (#0) and the higher order mode (#4), so that in the frequency range of the fundamental mode, mini-gaps so-called mini-stopbands (MSB)[34,35] appear.

Mode coupling between the defect modes could transfer the energy from the fundamental guided mode to the high-order modes which propagate backward with large losses. Therefore, transmission-dip can be observed in the transmission spectra in Fig. 4(b). Here, the transmission-dip is simulated under the two fabricated lattice constants. As seen, transmission-dip shows a red-shift of ~40 nm while the lattice constant increases from 412 nm to 425 nm.

The transmission spectra of W3 PCWs in InP heterostructure with 1.3μm-MQWs are measured with an auto-coupling alignment system and shown in Fig. 5. The shape and position of the transmission-dips are in good agreement with the theoretical predictions shown in Fig. 4(b), except the transmission drop in the highlighted region, where 1.3 μm-MQWs exhibit strong nonlinear absorption response to optical power. In addition, transmission-dip about 17 dB is obtained in the fabricated PCW, while the length is only about 17 μm ($L = 40a$). This transmission performance of good structure-dependent transmission-dip and large transmission extinction with a short PCW length clearly demonstrate the high etching quality of our process.

B. Measurement of micro-photoluminescence (μ-PL)

As known, poor surface states control by induced damages during etching will result in a wide photoluminescence (PL) spectrum, typically much wider than for the corresponding active materials, and thus poor light emission efficiency.[36] Therefore, to further determine the fabrication quality for active devices, μ-PL measurements of the etched W3 PCWs are performed at room temperature. Figure 6 shows the normalized PL for the InP heterostructure wafer and the two samples of the etched

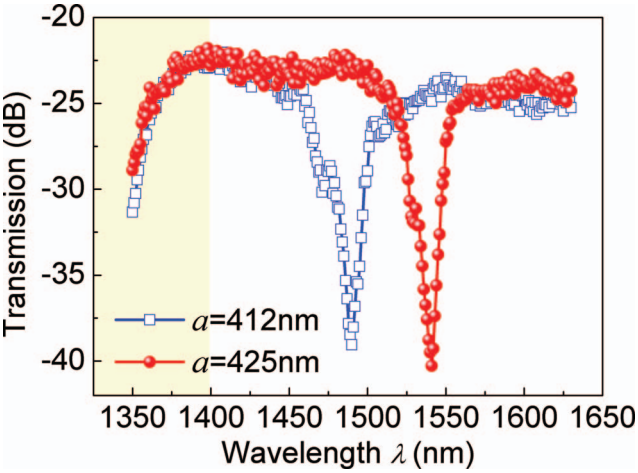

FIG. 5. Measured transmission spectra of W3 PCWs in InP heterostructure with 1.3μm-MQWs. The highlighted region is the span of MQWs absorption.

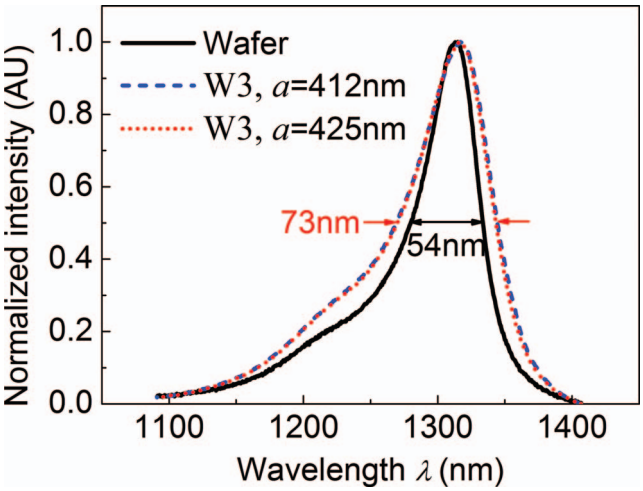

FIG. 6. Micro-photoluminescence (μ-PL) spectra for the InP heterostructure wafer with 1.3μm-MQWs and two samples of the fabricated W3 PCWs with etching condition given in Table I.

W3 PCWs with lattice period of 412 nm and 425 nm. The PL peak of the wafer originating from the InGaAsP-MQWs was narrowest with full width at half maximum (FWHM) of 54 nm around 1.30 μm. Compared to that of the wafer, the increase of the PL linewidth for the etched samples is only 19 nm, which is smaller than the widening of 35 nm reported in Ref. 36 at the condition of no chemical post-treatment. With further post-treatments,[11,36] we believe that superior surface quality could be produced by our etching process.

IV. CONCLUSIONS

For high-quality and high-aspect-ratio etching of ultra-small feature size patterns in InP material, we investigate the impact of process pressures on ICP etching profiles. We show that process pressures play a key role in deep etching for small features. In our case, due to using the low pressure of 0.05 Pa, etch depth up to 3.5 μm and 1.8 μm is achieved for the holes with diameter of 200 nm and slots of ~40 nm, respectively. The latter corresponds to an aspect-ratio as high as 45, which is the best-reported result up to now for such ultra-narrow slots in InP heterostructure. Besides, the selectivity is about 14 for our etching condition, hence it is favourable for the deep etching

technology. In addition, etching quality is evaluated based on the transmission performance and the linewidth of μ–PL. In our measurement, both the large transmission-dip (17 dB) from a 17-μm-long W3 PCW and the small PL widening (19 nm) compared to the wafer demonstrate the high etching quality of our process. These promising results pave the way for the ultra-compact InP based optical devices of electrically pumped for future mono-/hetero-integrated photonic circuits.

ACKNOWLEDGMENT

This work was supported by the National Basic Research Program of China (No. 2011CBA00608, 2011CBA00303 and 2011CB301803), the National Natural Science Foundation of China (Grant No. 61036011 and 61036010), and China Postdoctoral Science Foundation. The authors would like to thank Mr. Daisuke Kinoshita and Mr. Jianhui Zhou of Samco Corporation for their support on dry etching equipment. The authors would also like to thank Dr. Fang Liu for his valuable discussions.

[1] S. Matsuo, A. Shinya, T. Kakitsuka, K. Nozaki, T. Segawa, T. Sato, Y. Kawaguchi, and M. Notomi, Nat. Photonics **4**, 648 (2010).
[2] Y. Halioua, A. Bazin, P. Monnier, T. J. Karle, I. Sagnes, G. Roelkens, D. Van Thourhout, F. Raineri, and R. Raj, J. Opt. Soc. Am. B **27**, 2146 (2010).
[3] J. Kim, A. Shinya, K. Nozaki, H. Taniyama, C. H. Chen, T. Sato, S. Matsuo, and M. Notomi, Opt. Express **20**, 11643 (2012).
[4] M. Notomi, A. Shinya, K. Nozaki, T. Tanabe, S. Matsuo, E. Kuramochi, T. Sato, H. Taniyama, and H. Sumikura, IET Circuits Devices & Systems **5**, 84 (2011).
[5] S. G. Johnson, S. H. Fan, P. R. Villeneuve, J. D. Joannopoulos, and L. A. Kolodziejski, Phys. Rev. B **60**, 5751 (1999).
[6] E. Chow, S. Y. Lin, S. G. Johnson, P. R. Villeneuve, J. D. Joannopoulos, J. R. Wendt, G. A. Vawter, W. Zubrzycki, H. Hou, and A. Alleman, Nature **407**, 983 (2000).
[7] R. Kappeler, P. Kaspar, and H. Jackel, J. Lightwave Technol. **29**, 3156 (2011).
[8] A. Larrue, D. Belharet, P. Dubreuil, S. Bonnefont, O. Gauthier-Lafaye, A. Monmayrant, F. Lozes-Dupuy, and S. Moumdji, J. Vac. Sci. Technol. B **29**, 021006 (2011).
[9] B. Ellis, M. A. Mayer, G. Shambat, T. Sarmiento, J. Harris, E. E. Haller, and J. Vuckovic, Nat. Photonics **5**, 297 (2011).
[10] G. Shambat, B. Ellis, A. Majumdar, J. Petykiewicz, M. A. Mayer, T. Sarmiento, J. Harris, E. E. Haller, and J. Vuckovic, Nat. Commun. **2**, 539 (2011).
[11] N. Shahid, S. Naureen, M. Y. Li, M. Swillo, and S. Anand, J. Vac. Sci. Technol. B **29**, 031202 (2011).
[12] P. Strasser, R. Wuest, F. Robin, D. Erni, and H. Jackel, J. Vac. Sci. Technol. B **25**, 387 (2007).
[13] M. Mulot, S. Anand, M. Swillo, M. Qiu, B. Jaskorzynska, and A. Talneau, J. Vac. Sci. Technol. B **21**, 900 (2003).
[14] M. V. Kotlyar, L. O'Faolain, R. Wilson, and T. F. Krauss, J. Vac. Sci. Technol. B **22**, 1788 (2004).
[15] V. R. Almeida, Q. F. Xu, C. A. Barrios, and M. Lipson, Opt. Lett. **29**, 1209 (2004).
[16] Q. M. Quan, I. Bulu, and M. Loncar, Phys. Rev. A **80**, 011810 (2009).
[17] X. Wang, C. Lin, S. Chakravarty, J. Luo, A. K. Y. Jen, and R. T. Chen, Opt. Lett. **36**, 882 (2011).
[18] W. C. Lai, S. Chakravarty, X. L. Wang, C. Y. Lin, and R. T. Chen, Opt. Lett. **36**, 984 (2011).
[19] M. G. Scullion, A. Di Falco, and T. F. Krauss, Biosens. Bioelectron. **27**, 101 (2011).
[20] M. Eichenfield, R. Camacho, J. Chan, K. J. Vahala, and O. Painter, Nature **459**, 550 (2009).
[21] S. Kita, S. Hachuda, S. Otsuka, T. Endo, Y. Imai, Y. Nishijima, H. Misawa, and T. Baba, Opt. Express **19**, 17683 (2011).
[22] J. T. Robinson, C. Manolatou, L. Chen, and M. Lipson, Phys. Rev. Lett. **95**, 143901 (2005).
[23] M. Mulot, S. Anand, R. Ferrini, B. Wild, R. Houdre, J. Moosburger, and A. Forchel, J. Vac. Sci. Technol. B **22**, 707 (2004).
[24] A. Berrier, M. Mulot, S. Anand, A. Talneau, R. Ferrini, and R. Houdre, J. Vac. Sci. Technol. B **25**, 1 (2007).
[25] F. Pommereau, L. Legouezigou, S. Hubert, S. Sainson, J. P. Chandouineau, S. Fabre, G. H. Duan, B. Lombardet, R. Ferrini, and R. Houdre, J. Appl. Phys. **95**, 2242 (2004).
[26] K. Y. Cui, Y. D. Huang, G. Y. Zhang, Y. Z. Li, X. Tang, X. Y. Mao, Q. Zhao, W. Zhang, and J. D. Peng, Appl. Phys. Lett. **95**, 191901 (2009).
[27] K. Y. Cui, Q. Zhao, X. Feng, Y. D. Huang, Y. Z. Li, D. Wang, and W. Zhang, Appl. Phys. Lett. **100**, 201102 (2012).
[28] N. Shahid, N. Speijcken, S. Naureen, M. Y. Li, M. Swillo, and S. Anand, Appl. Phys. Lett. **98**, 081112 (2011).
[29] M. Qiu, M. Swillo, M. Mulot, S. Anand, B. Jaskorzynska, A. Karlsson, and L. Thylén, Proc. SPIE **4905**, 22 (2002).
[30] T. Yoshikawa, S. Kohmoto, M. Anan, N. Hamao, M. Baba, N. Takado, Y. Sugimoto, M. Sugimoto, and K. Asakawa, Jpn J. Appl. Phys. **31**, 4381 (1992).
[31] T. Ide, J. Hashimoto, K. Nozaki, E. Mizuta, and T. Baba, Jpn J. Appl. Phys. **45**, L102 (2006).
[32] A. Matsutani, H. Ohtsuki, S. Muta, F. Koyama, and K. Iga, Jpn J. Appl. Phys. **40**, 1528 (2001).
[33] K. Y. Cui, X. Feng, Y. D. Huang, Q. Zhao, Z. L. Huang, and W. Zhang, Appl. Phys. Lett. **101**, 151110 (2012).
[34] S. Olivier, H. Benisty, C. Weisbuch, C. Smith, T. F. Krauss, and R. Houdre, Opt. Express **11**, 1490 (2003).
[35] K. Y. Cui, Y. D. Huang, W. Zhang, and J. D. Peng, J. Lightwave Technol. **26**, 1492 (2008).
[36] H. Wang, M. H. Sun, K. Ding, M. T. Hill, and C. Z. Ning, Nano Lett. **11**, 1646 (2011).